



Cite this: *Chem. Commun.*, 2016, 52, 7680

Received 14th February 2016,  
Accepted 18th May 2016

DOI: 10.1039/c6cc01373b

www.rsc.org/chemcomm

## Stabilization of a Zn(II) hydrosulfido complex utilizing a hydrogen-bond accepting ligand†

Matthew D. Hartle,<sup>a</sup> Mayra Delgado,<sup>b</sup> John D. Gilbertson\*<sup>b</sup> and Michael D. Pluth\*<sup>a</sup>

**Hydrogen sulfide (H<sub>2</sub>S) has gained recent attention as an important biological analyte that interacts with bioinorganic targets. Despite this importance, stable H<sub>2</sub>S or HS<sup>−</sup> adducts of bioinorganic metal complexes remain rare due to the redox activity of sulfide and its propensity to form insoluble metal sulfides. We report here reversible coordination of HS<sup>−</sup> to Zn(didpa)Cl<sub>2</sub>, which is enabled by an intramolecular hydrogen bond between the zinc hydrosulfido product and the pendant tertiary amine of the didpa ligand.**

Although historically known for its malodour and toxicity, hydrogen sulfide (H<sub>2</sub>S) has joined nitric oxide (NO) and carbon monoxide (CO) as a physiologically important gasotransmitter.<sup>1</sup> Complicating its reactivity with different bioinorganic targets, H<sub>2</sub>S has multiple protonation states, participates in complex redox chemistry, and is highly metallophilic.<sup>2,3</sup> For example, the high affinity between zinc and sulfide ( $\Delta G_f^\circ = -48.11$  kcal mol<sup>−1</sup>, sphalerite)<sup>4</sup> limits generation of stable sulfide-ligated products, but has also been leveraged as a sulfide sequestration strategy in quantification and detection methods.<sup>5,6</sup> Consequently, stable zinc hydrosulfido complexes remain rare,<sup>7–11</sup> with reported examples including (tris)pyrazolylborate zinc hydrosulfide (TpZnSH) complexes, supported by the steric protection from the Tp ligand.<sup>7,8</sup> Complementing the use of steric protection, secondary-coordination sphere interactions have also been used to stabilize metal-sulfide species with other metals, such as iron.<sup>12</sup> Additionally, these stabilizing forces are hypothesized to be important in the mechanism of carbonyl sulfide fixation by carbonic anhydrase.<sup>13,14</sup>

Toward increasing our understanding of the solution state stabilization of metal hydrosulfido complexes, we viewed that a ligand scaffold with a pendant hydrogen-bond (H-bond) acceptor would provide a viable scaffold for Zn-SH stabilization.

We noted that the pyridinediimine (PDI) ligand scaffold didpa ( $[(2,6\text{-}^i\text{PrC}_6\text{H}_3)(\text{N}=\text{CMe})(\text{N}(^i\text{Pr})_2\text{C}_2\text{H}_4)(\text{N}=\text{CMe})\text{C}_5\text{H}_3\text{N}]$ ) has been demonstrated to function as an H-bond donor when the pendant diisopropylamine is protonated and used to stabilize metal halogen hydrogen bonds (MHHBs), with calculated MHHB strengths of  $\sim 6$  kcal mol<sup>−1</sup> for [Zn(Hdidpa)Cl<sub>2</sub>][PF<sub>6</sub>].<sup>15</sup> Additionally, the protonated form of the ligand can also function as an H-bond donor to stabilize rare Fe-OH species.<sup>16</sup> Although ligands displaying hydrogen-bond donors in the secondary coordination sphere are now frequently used in bioinorganic model complexes,<sup>17,18</sup> hydrogen-bond accepting ligands are rare.<sup>19–23</sup> On the basis of these properties, we reasoned that the didpa ligand could function as an H-bond acceptor in its neutral form to provide a suitable ligation environment for metal hydrosulfido stabilization.

Treatment of Zn(didpa)Cl<sub>2</sub> (**1**) with H<sub>2</sub>S gas failed to produce any reaction, however treatment of **1** with NBu<sub>4</sub>SH<sup>24</sup> in either CH<sub>2</sub>Cl<sub>2</sub> (Fig. 1) or MeCN (Fig. S1, ESI†) resulted in a significant change in the UV-Vis spectrum. In CH<sub>2</sub>Cl<sub>2</sub> the shoulder at 313 nm decreased in intensity with a concomitant increase in absorbance at 280 nm and a well-anchored isosbestic point at 296 nm upon addition of HS<sup>−</sup>. A Job plot was consistent with

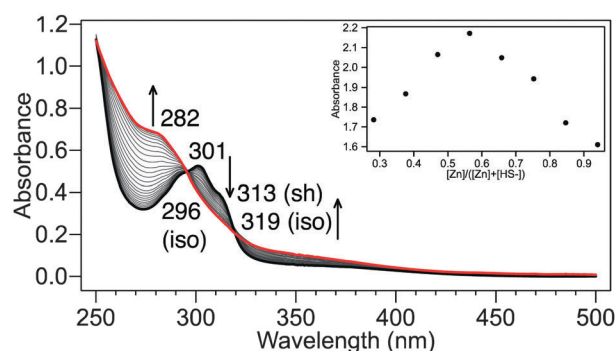


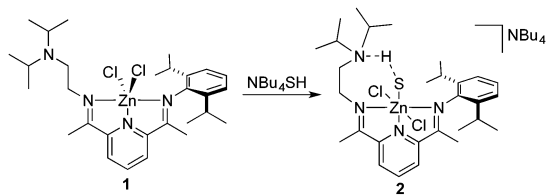
**Fig. 1** Titration of Zn(didpa)Cl<sub>2</sub> (87.3 μM, CH<sub>2</sub>Cl<sub>2</sub>, black) with NBu<sub>4</sub>SH (0.1 equiv. increments up to 6 equiv., red). The inset shows the Job plot of **1** with NBu<sub>4</sub>SH in MeCN at a total concentration of 420 μM. The observed break is consistent with 1 : 1 binding.

<sup>a</sup> Department of Chemistry and Biochemistry, Materials Science Institute, Institute of Molecular Biology, University of Oregon, Eugene, Oregon 97403, USA. E-mail: pluth@uoregon.edu

<sup>b</sup> Department of Chemistry, Western Washington University, Bellingham, WA, 98225, USA. E-mail: John.gilbertson@wwu.edu

† Electronic supplementary information (ESI) available: Experimental details, additional spectroscopic and NMR data. See DOI: 10.1039/c6cc01373b





**Scheme 1** Reaction of  $\text{Zn}(\text{didpa})\text{Cl}_2$  (**1**) with  $\text{NBu}_4\text{SH}$  to generate hydro-sulfide adduct **2**.

1 : 1 binding of  $\text{HS}^-$  to **1** (Fig. 1, inset). In addition, titration with  $\text{HO}^-$  resulted in 1 : 1 binding (Fig. S13, ESI $^\dagger$ ). Based on these results, and because chloride abstraction was not required for  $\text{HS}^-$  binding, we propose that  $\text{HS}^-$  binds to **1** to generate six-coordinate  $[\text{Zn}(\text{didpa})\text{Cl}_2\text{SH}]^-$  (**2**, Scheme 1). All attempts to grow single crystals suitable for X-ray structural determination of **2** resulted in precipitation of a white amorphous powder after prolonged standing. Supporting the associative formation of a six-coordinate product, titration of **1** with excess  $\text{Cl}^-$  showed similar spectral changes by UV-Vis spectroscopy (Fig. S3 and S4, ESI $^\dagger$ ), and the Job plot was consistent with 1 : 1  $\text{Cl}^-$  binding (Fig. S12, ESI $^\dagger$ ). Attempts to isolate and crystallize the six-coordinate 1 : 1 adduct of  $\text{Cl}^-$  and **1** with a range of different  $\text{Cl}^-$  sources ( $\text{Bu}_4\text{NCl}$ ,  $\text{Ph}_4\text{NCl}$ ,  $\text{PPNCl}$ ) resulted in simple recrystallization of the starting chloride salt and **1**, presumably due to the reversibility of the process.

To gain further insights into the  $\text{HS}^-$  binding, we used  $^1\text{H}$  NMR spectroscopy to investigate the stability of **2** and the role of hydrogen-bonding in the complex. Treatment of **1** with 1.5 equiv. of  $\text{NBu}_4\text{SH}$  in  $\text{CD}_3\text{CN}$  resulted in significant changes in the  $^1\text{H}$  NMR spectrum. The resultant spectrum did not match that of the free ligand,<sup>15</sup> suggesting that addition of  $\text{HS}^-$  does not remove Zn from the didpa ligand (Fig. 2). Upon  $\text{HS}^-$  addition, the pyridine and other aryl resonances of **1** shifted significantly in a pattern consistent with loss of free rotation of the 2,6-diisopropylphenyl group of the ligand. Similarly, the isopropyl resonance at 1.00 ppm, corresponding to the isopropyl methyl groups of the pendant amine, shifts downfield and bifurcates. Each of these spectral changes indicated a significant change in

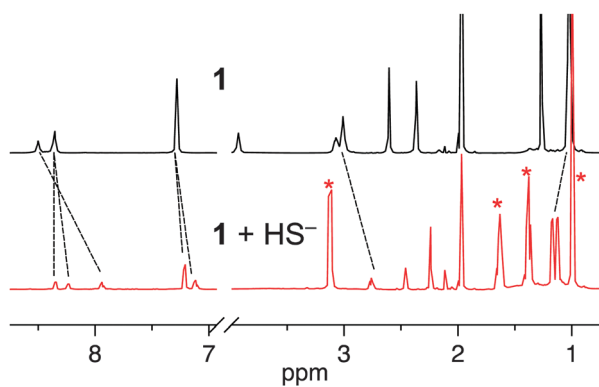


**Fig. 2**  $^1\text{H}$  NMR spectra of **1** (11.8 mM in  $\text{CD}_3\text{CN}$ ) before (top, black) and after (bottom, red) addition of 1.5 equiv. of  $\text{NBu}_4\text{SH}$ . Peaks denoted with a (\*) correspond to the  $\text{NBu}_4^+$  counterion.

the primary coordination sphere of the zinc and are consistent with formation of a six-coordinate complex in which the  $\text{Zn-SH}$  moiety is hydrogen bonded to the pendant diisopropylamine (Scheme 1).

Low temperature  $^1\text{H}$  NMR investigations provided additional information about the structural flexibility of the scaffold and the presence of the coordinated hydrosulfide. Although we were unable to observe an appreciable signal corresponding to the coordinated  $\text{HS}^-$  at room temperature, we expected that lowering the temperature would not only enable  $\text{HS}^-$  observation, but also lock the conformation of the ethylene backbone of the ligand. Consistent with these expectations, cooling to  $-35^\circ\text{C}$  in  $\text{CD}_3\text{CN}$  resulted in the appearance of a new resonance at 11.05 ppm, matching the general chemical shift expected for partial protonation of the nitrogen as an H-bond acceptor (Fig. 3).<sup>25</sup> For comparison, the  $^1\text{H}$  NMR spectrum of the previously reported  $[\text{Zn}(\text{Hdidpa})\text{Cl}_2][\text{PF}_6]$  displays an N-H resonance at 8.50 ppm in  $\text{CD}_2\text{Cl}_2$  due to the protonated diisopropylamine of the didpa ligand acting as an H-bond donor and forming an intramolecular MHHB with a chloride ligand.<sup>15</sup> The downfield shift observed for **2** is consistent with the diisopropylamine acting as an H-bond acceptor, likely accepting a hydrogen bond from the Zn-ligated SH moiety.<sup>26</sup>

Additionally, we observed that the broad peak centered at 3.6 ppm corresponding to the ethylene bridge decoalesced upon cooling. The presence of the internal hydrogen bond between the sulfhydryl group and the tertiary amine significantly limits the flexibility of the secondary coordination sphere, resulting in a sharpening in the signal produced by the ethylene linker, methine protons, and methyl groups (Fig. S8, ESI $^\dagger$ ). Supporting the presence of an intramolecular SH hydrogen bond, a  $^1\text{H}$  NOESY experiment at  $-35^\circ\text{C}$  revealed cross peaks between the SH and the ethylene, methine, and methyl signals of the tertiary amine linker (Fig. S5, ESI $^\dagger$ ).

Although the  $\text{N}\cdots\text{HS}$  interaction was not observed by solution FTIR, we note that the N-H stretch involved in hydrogen bonding in the  $[\text{Zn}(\text{Hdidpa})\text{Cl}_2][\text{PF}_6]$  system is also absent in solution FTIR spectra.<sup>15</sup> The N-H stretch in the  $\text{N}\cdots\text{HS}$  moiety is likely severely broadened or obscured, which is common in many hydrogen bonding systems.<sup>25</sup>

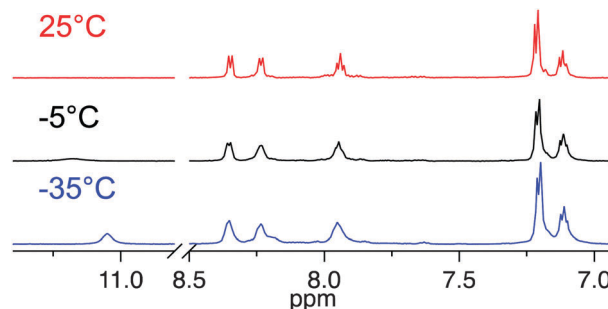


**Fig. 3** Variable temperature  $^1\text{H}$  NMR spectra of 11.4 mM  $\text{Zn}(\text{didpa})\text{Cl}_2$  and 1.5 equiv.  $\text{NBu}_4\text{SH}$  in  $\text{CD}_3\text{CN}$ . Cooling to  $-35^\circ\text{C}$  results in sharpening and an upfield shift of the broad SH peak to 11.05 ppm. See Fig. S9 (ESI $^\dagger$ ) for an expanded spectrum of the SH peak.



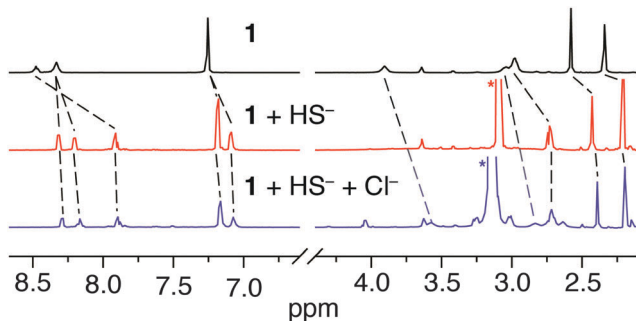
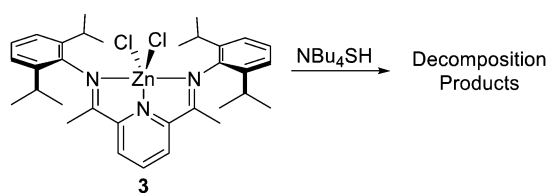


Fig. 4  $^1\text{H}$  NMR spectrum of 10.3 mM **1** (black), upon addition of 1.5 equiv. of  $\text{NBu}_4\text{SH}$  (red) is characteristic for **2**. Addition of 20 equiv. of  $\text{NBu}_4\text{Cl}$  produces the spectrum characteristic of the  $\text{Cl}^-$  adduct.

To demonstrate the reversibility of **2**, and to provide evidence for the formation of a six-coordinate complex, we performed a displacement experiment by  $^1\text{H}$  NMR. Treatment of **1** with 1.5 equiv. of  $\text{NBu}_4\text{SH}$  resulted in the formation of **2** with characteristic shifts in the aryl peaks, and broad resonance at 3.6 ppm (Fig. 4). Upon addition of 20 equiv. of  $\text{NBu}_4\text{Cl}$ , the aryl protons maintained the same configuration; however, the broad absorbance at 3.6 ppm resolved, characteristic of the  $\text{Cl}^-$  adduct of **1** (Fig. S6, ESI $^\dagger$ ).<sup>27</sup>

To further determine whether the internal hydrogen-bond was necessary for stabilization of the Zn-SH product, we also titrated a Zn-pyridinediimine compound which does not possess the pendant amine hydrogen-bond acceptor (Scheme 2). Upon addition of 0.5 equiv. of  $\text{HS}^-$  to a solution of  $\text{Zn}(\text{Pr}^i\text{PDI})\text{Cl}_2$  (**3**) ( $\text{Pr}^i\text{PDI} = 2,6-(2,6\text{-}^i\text{Pr}_2\text{C}_6\text{H}_3\text{N}=\text{CMe})_2\text{C}_5\text{H}_3\text{N}$ ) a white precipitate (ZnS) was immediately observed, along with a significant change in the NMR spectrum. The shifts in the NMR spectrum and formation of precipitate continued until 1 equiv. of  $\text{HS}^-$  was added, after which no more changes were observed (Fig. S11, ESI $^\dagger$ ). The resultant solid was isolated, washed with acetonitrile to remove any excess free sulfide, then acidified and subjected to the methylene blue assay, which provided a positive response for acid-labile sulfur and was consistent with ZnS formation.<sup>28</sup> These data illustrate the importance of the hydrogen-bond acceptor in the



Scheme 2 Reaction of **3** with  $\text{NBu}_4\text{SH}$  shows decomposition, demonstrating the importance of the H-bond acceptor in **2**.

stabilization of the zinc-sulfido complex, as the pendant amine in **1** is vital in this system.

In conclusion, we have shown the stabilization of a rare synthetic zinc hydrosulfide complex stabilized by a hydrogen bond accepting ligand. Removal of the hydrogen bonding ability of the ligand resulted in decomposition and ZnS precipitation, highlighting the importance of the second coordination sphere in stabilizing the zinc hydrosulfido adduct.

This work was supported by CAREER Awards from the National Science Foundation (CHE-1454747 to MDP, CHE-1255570 to JDG) and the Sloan Foundation (MDP). The NMR facilities at the University of Oregon are supported by NSF/ARRA (CHE-0923589).

## Notes and references

- 1 R. Wang, *Physiol. Rev.*, 2012, **92**, 791–896.
- 2 M. D. Hartle, S. K. Sommer, S. R. Dietrich and M. D. Pluth, *Inorg. Chem.*, 2014, **53**, 7800–7802.
- 3 C. C. Tsou, W. C. Chiu, C. H. Ke, J. C. Tsai, Y. M. Wang, M. H. Chiang and W. F. Liaw, *J. Am. Chem. Soc.*, 2014, **136**, 9424–9433.
- 4 P. Patnaik, *Handbook of Inorganic Chemicals*, McGraw-Hill, New York, 2002.
- 5 J. K. Fogo and M. Popowsky, *Anal. Chem.*, 1949, **21**, 732–734.
- 6 E. Galardon, A. Tomas, P. Roussel and I. Artaud, *Dalton Trans.*, 2009, 9126–9130.
- 7 M. Rombach and H. Vahrenkamp, *Inorg. Chem.*, 2001, **40**, 6144–6150.
- 8 M. Ruf and H. Vahrenkamp, *Inorg. Chem.*, 1996, **35**, 6571–6578.
- 9 M. M. Morlok, K. E. Janak, G. Zhu, D. A. Quarless and G. Parkin, *J. Am. Chem. Soc.*, 2005, **127**, 14039–14050.
- 10 N. G. Spiropoulos, E. A. Standley, I. R. Shaw, B. L. Ingalls, B. Diebels, S. V. Krawczyk, B. F. Gherman, A. M. Arif and E. C. Brown, *Inorg. Chim. Acta*, 2012, **386**, 83–92.
- 11 S. Kuwata and M. Hidai, *Coord. Chem. Rev.*, 2001, **213**, 211–305.
- 12 E. Galardon, T. Roger, P. Deschamps, P. Roussel, A. Tomas and I. Artaud, *Inorg. Chem.*, 2012, **51**, 10068–10070.
- 13 J. Notni, S. Schenk, G. Protoschill-Krebs, J. Kesselmeier and E. Anders, *ChemBioChem*, 2007, **8**, 530–536.
- 14 F. Namuswe and J. M. Berg, *J. Inorg. Biochem.*, 2012, **111**, 146–149.
- 15 M. Delgado, S. K. Sommer, S. P. Swanson, R. F. Berger, T. Seda, L. N. Zakharov and J. D. Gilbertson, *Inorg. Chem.*, 2015, **54**, 7239–7248.
- 16 A. J. Kendall, L. N. Zakharov and J. D. Gilbertson, *Inorg. Chem.*, 2010, **49**, 8656–8658.
- 17 A. S. Borovik, *Acc. Chem. Res.*, 2005, **38**, 54–61.
- 18 S. A. Cook and A. S. Borovik, *Acc. Chem. Res.*, 2015, **48**, 2407–2414.
- 19 Y. J. Park, N. S. Sickerman, J. W. Ziller and A. S. Borovik, *Chem. Commun.*, 2010, **46**, 2584–2586.
- 20 N. S. Sickerman, Y. J. Park, G. K. Ng, J. E. Bates, M. Hilbert, J. W. Ziller, F. Furche and A. S. Borovik, *Dalton Trans.*, 2012, **41**, 4358–4364.
- 21 Z. Shirin and C. J. Carrano, *Polyhedron*, 2004, **23**, 239–244.
- 22 C. M. Moore and N. K. Szymczak, *Dalton Trans.*, 2012, **41**, 7886–7889.
- 23 E. M. Matson, J. A. Bertke and A. R. Fout, *Inorg. Chem.*, 2014, **53**, 4450–4458.
- 24 M. D. Hartle, D. J. Meiningner, L. N. Zakharov, Z. J. Tonzetich and M. D. Pluth, *Dalton Trans.*, 2015, **44**, 19782–19785.
- 25 T. Steiner, *Angew. Chem., Int. Ed.*, 2002, **41**, 48–76.
- 26 B. Brzeninski and G. Zundel, *J. Mol. Struct.*, 1982, **84**, 205–211.
- 27 Based on the number of equivalents of  $\text{HS}^-$  required to displace the bound  $\text{Cl}^-$ , we estimate that the binding affinity of  $\text{HS}^-$  for  $\text{Zn}(\text{didpa})\text{Cl}_2$  is similar and not more than  $10\times$  greater than that of  $\text{Cl}^-$ . See Fig. S3 (ESI $^\dagger$ ).
- 28 X. Shen, C. B. Pattillo, S. Pardue, S. C. Bir, R. Wang and C. G. Kevill, *Free Radical Biol. Med.*, 2011, **50**, 1021–1031.

